Limits on Spin-Charge Separation from $h/2e$ Fluxoids in Very Underdoped $YBa_2Cu_3O_{6+x}$

J. C. Wynn,[1] D. A. Bonn,[2] B. W. Gardner,[1] Yu-Ju Lin,[1] Ruixing Liang,[2] W. N. Hardy,[2] J. R. Kirtley,[3] and K. A. Moler[1,*]

[1]*Geballe Laboratory for Advanced Materials, Stanford University, Stanford, California 94305*

[2]*Department of Physics and Astronomy, University of British Columbia, Vancouver, BC Canada V6T 1Z1*

[3]*IBM T. J. Watson Research Center, Yorktown Heights, New York 10598*

(Received 12 May 2001; published 16 October 2001)

Magnetic flux in superconductors is usually quantized in units of $h/2e$. Here we report scanning SQUID and scanning Hall probe studies of single fluxoids in high purity $YBa_2Cu_3O_{6.35}$ crystals ($T_c \lesssim 13$ K), extending flux quantization studies to a region of the cuprate phase diagram where the superfluid density is sufficiently low that novel behavior has been predicted. Some scenarios in which superconductivity results from spin-charge separation predict h/e fluxoids in materials with low superfluid density. Our observations of only $h/2e$ fluxoids set limits on these theories.

DOI: 10.1103/PhysRevLett.87.197002 PACS numbers: 74.25.Ha, 74.60.–w, 74.72.Bk

Despite intense effort over the past 15 years, agreement on the mechanism of superconductivity in the cuprates has not been reached. The cuprate phase diagram is sketched in Fig. 1(a). Many theories of cuprate superconductivity make their sharpest predictions for very underdoped samples, where the superfluid density is lowest. A key feature of superconductivity is magnetic flux quantization. Experimentally, flux is found to be quantized in units of $h/2e$ in both conventional superconductors [1] and near-optimally doped cuprates [2], but flux quantization in high quality samples of the cuprate superconductor $YBa_2Cu_3O_{6+x}$ (YBCO) in the very underdoped region has not previously been studied.

We report magnetic imaging experiments on four single crystals of $YBa_2Cu_3O_{6.35}$ with critical temperatures (T_c) of 11–13 K. This work was motivated by the general importance of flux quantization, and by specific scenarios in which superconductivity results from spin-charge separation (SCS). In conventional superconductivity, electrons form Cooper pairs (charge $2e$ bosons), giving $h/2e$ flux quanta. In SCS the electron *fractionalizes* into a chargeless spin-1/2 fermion (called a *spinon*) and a spinless charge e boson (called a *holon* or *chargon*) [3]. Thus h/e flux quantization would naively be expected, because a charge e particle circling an h/e fluxoid acquires a 2π phase shift. SCS theories do in fact allow $h/2e$ fluxoids [4], but it has long been recognized that SCS may lead to h/e fluxoids, specifically in samples with low superfluid density and a high energy scale for SCS [5–8] [Fig. 1(a)]. Senthil and Fisher introduce an excitation called a *vison* [9] which provides a π phase shift to a circling chargon, thereby enabling $h/2e$ fluxoids at an energy cost of $E_{\text{vison}} \approx k_B T^*$, where T^* is the pseudogap temperature [8]. The balance of superfluid energy, fluxoid core energy, and vison energy determines whether h/e or $h/2e$ fluxoids are preferred. It should be remarked that the meaning of SCS and the generality of the Senthil-Fisher approach remain under discussion [10].

We imaged over 170 fluxoids in the $YBa_2Cu_3O_{6.35}$ samples with scanning superconducting quantum interference device (SQUID) microscopy and scanning Hall probe microscopy, both of which measure magnetic flux quantitatively. The Hall probe measurements are somewhat noisier but cover a wider temperature range and have higher spatial resolution. All the observed fluxoids carried a single conventional flux quantum, $h/2e$, within

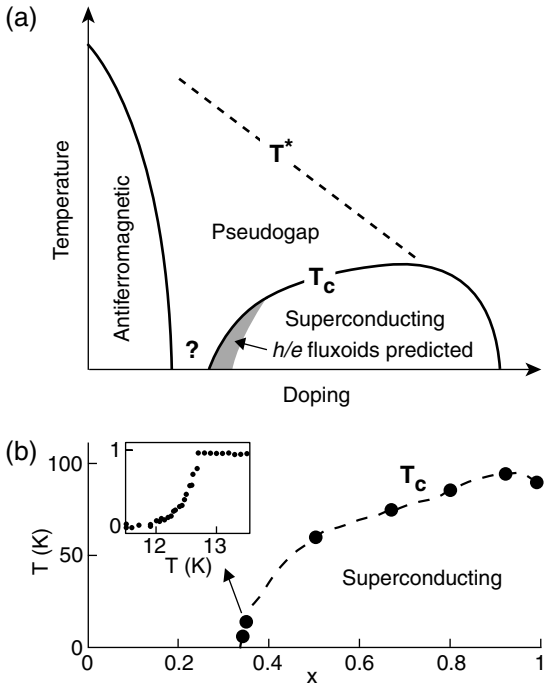

FIG. 1. (a) Idealized temperature-doping phase diagram of the cuprate superconductors. The question mark indicates a poorly understood region. Samples with doping below that which gives the maximum T_c are called *underdoped*. The shaded area qualitatively indicates where h/e fluxoids are predicted in theories of spin-charge separation [5–8]. (b) T_c as a function of oxygen content in $YBa_2Cu_3O_{6+x}$ crystals [12]. Inset: magnetic transition of a $YBa_2Cu_3O_{6.35}$ crystal measured locally with a Hall probe in an applied ac field of 0.06 mT. The vertical axis is the magnetic field measured by the Hall probe normalized by the applied field.

 0031-9007/01/87(19)/197002(4)$15.00

experimental error. These results set a semiquantitative upper limit on the energy scale for spin-charge separation which is much lower than predicted.

Our low-T_c samples of $YBa_2Cu_3O_{6+x}$ are the product of recent improvements in crystalline perfection with the use of $BaZrO_3$ crucibles for crystal growth [11,12]. Figure 1(b) shows T_c as a function of the oxygen content that sets the doping in these high purity crystals. The lowest T_c's are found at about $x = 0.35$, produced by annealing crystals at 900 °C in flowing oxygen. After this first anneal the crystals were sealed in a quartz ampoule, together with pieces of a $YBa_2Cu_3O_{6.35}$ ceramic, and heated to 580 °C to homogenize the oxygen content. After quenching to room temperature, these samples are not superconducting, but annealing near room temperature for a few weeks [13] allows the intercalated oxygen to order into CuO chains [12], producing samples with $T_c \approx 12$ K and $\Delta T_c \lesssim 2$ K [Fig. 1(b) inset]. The platelet-shaped crystals were 10–100 microns thick along the c axis and about 1 mm × 1 mm with the ab plane parallel to the surface [11,12].

Over 110 fluxoids in three single crystals of $YBa_2Cu_3O_{6.35}$ were studied with the scanning SQUID in the temperature range 2–7 K. The microscope and Nb SQUID have been described elsewhere [14]. The SQUID's 8 μm square pickup loop is aligned parallel to the sample surface at a height $z \approx 1.5$ μm. For comparison, fluxoids in crystals with $x = 0.50$ ($T_c \approx 60$ K) were also imaged. The apparent shape of the fluxoids is due primarily to the shape of the pickup loop [Fig. 2(a)].

The total flux carried by fluxoids in the SQUID images was determined by integration and fits. Integrating the signal from isolated fluxoids over a relatively large area of 1000 μm^2 yielded flux $\Phi = 0.9 \pm 0.2$ $h/2e$. The quoted errors include conservative estimates of uncertainties in the effective SQUID pickup loop area, the distance calibration of the scanner, and the background determination. Throughout this paper, flux values rounded to the nearest tenth are representative of the analysis of numerous fluxoids. The total flux was also determined by fitting a model of the fluxoid magnetic field. For a half-infinite sample oriented along the c axis, in the limit $(r^2 + z^2) \gg \lambda_{ab}^2$ where $\vec{r} = (x, y)$ is the distance from the fluxoid center, the field is closely approximated by a monopole [15,16],

$$B_z(r,z) = \frac{\Phi}{2\pi} \frac{z + \lambda_{ab}}{[r^2 + (z + \lambda_{ab})^2]^{3/2}}, \qquad (1)$$

where $B_z(r,z)$ is the magnetic field perpendicular to the surface of the sample. [For our very underdoped YBCO measurements, the limit $(r^2 + z^2) \gg \lambda_{ab}^2$ is not strictly valid for small r, but comparison to a full model [17,18] indicates that the approximation remains acceptable [19].] The measured signal is the total magnetic flux through the SQUID pickup loop, treated as a perfect 8 μm × 8 μm square for fitting. Cross sections through the fluxoid center were fit with free parameters ($z + \lambda_{ab}$), total flux Φ, and a linear background [Fig. 2(b)]. The fits consistently gave $\Phi = 1.0 \pm 0.1$ $h/2e$ for fluxoids in the $x = 0.35$ and $x = 0.50$ crystals.

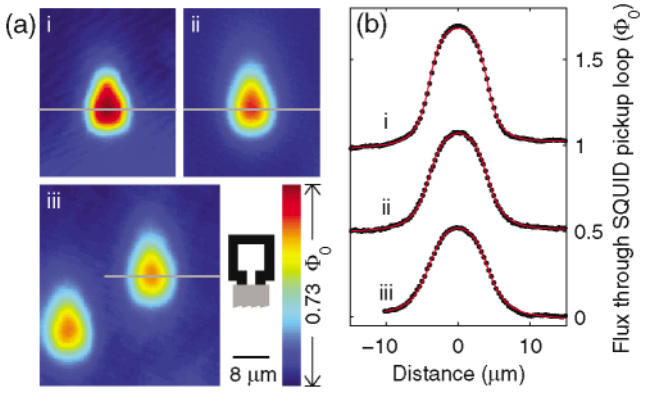

FIG. 2 (color). (a) Scanning SQUID microscopy of fluxoids in high purity $YBa_2Cu_3O_{6+x}$ crystals (i) at $T = 3.4$ K in an $x = 0.50$ ($T_c \approx 60$ K) crystal; (ii) at 2.1 K and (iii) at 6.3 K in an $x = 0.35$ ($T_c \approx 12$ K) crystal. The color scale corresponds to the flux through the SQUID pickup loop in units of $\Phi_0 = h/2e$. The teardrop shape is due to the pickup loop leads. Inset: sketch of the SQUID pickup loop drawn to the same scale. (b) Data (points) with fits (red lines) from image cross sections corresponding to the gray lines in (a), offset by 0.5 Φ_0 for clarity. The model is discussed in the text. Images in (a) and cross sections in (b) are displayed with a constant background subtracted. The fits gave (i) $z + \lambda_{ab} = 1.5 \pm 0.2$ μm and $\Phi = 1.00 \pm 0.07$ Φ_0, (ii) 2.0 ± 0.2 μm and 0.96 ± 0.07 Φ_0, and (iii) 2.3 ± 0.2 μm and 0.97 ± 0.07 Φ_0.

We also made scanning Hall probe [16] images of fluxoids in a crystal of $YBa_2Cu_3O_{6.35}$ with an onset T_c of 12.7 K [Fig. 1(b) inset], and for comparison and calibration, in a $YBa_2Cu_3O_{6.95}$ crystal with $T_c = 92$ K. Figure 3 shows images at 4.2 K after cooling in magnetic fields chosen to give desirable fluxoid densities in each crystal. The fluxoid images in the $x = 0.95$ crystal [Fig. 3(a)] appear to be resolution limited, consistent with the known low-temperature penetration depth in similar near-optimally

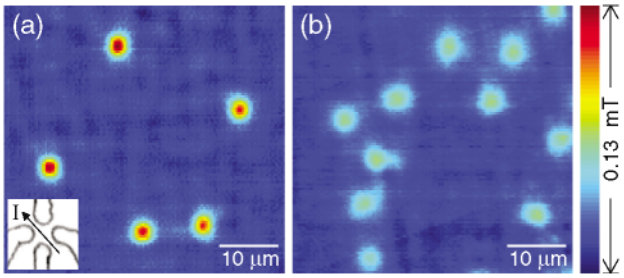

FIG. 3 (color). Scanning Hall probe images of $h/2e$ fluxoids in $YBa_2Cu_3O_{6+x}$ crystals at 4.2 K with line-by-line background subtraction. (a) In a nearly optimally doped sample with $x = 0.95$ and $T_c = 92$ K. Inset: the Hall probe at the same scale, with the direction of the ac current (I) as shown. (b) In a very underdoped sample with $x = 0.35$ and $T_c = 12.7$ K.

doped samples, $\lambda_{ab} \approx 0.16\ \mu$m [20]. Fits to the fluxoid images in that sample were therefore used to characterize the size and shape of the nominally 2 μm Hall probe [shown in Fig. 3(a) inset]. The images in Fig. 3 were obtained on adjacent, aligned, flat samples to ensure a constant $z \approx 1\ \mu$m.

Although the Hall probe had more background and less field sensitivity than the SQUID (making averaging necessary), the Hall probe was crucial for a thorough survey of fluxoids in the very underdoped samples, since h/e fluxoids should be most stable close to T_c [5–8] [Fig. 1(a)]. We imaged fluxoids formed after cooling just below the $T_c = 12.7$ K of the $YBa_2Cu_3O_{6.35}$ sample. This addressed a scenario in which energetically favored h/e fluxoids might not form if $h/2e$ fluxoids, which repel each other, were already present. Often we continued cooling and imaged the fluxoids for T as low as 3 K, and then again just below T_c. The fluxoid locations did not change with this temperature cycling below T_c, indicating that fluxoids neither split nor condensed, and thus that each carried an unchanging amount of flux at low temperatures up to at least 11 K, where we had insufficient sensitivity to resolve the fluxoids. One such cooling cycle is shown in Fig. 4. When cycled above T_c to 15 K and back down, fluxoids sometimes, but not always, formed at the same locations.

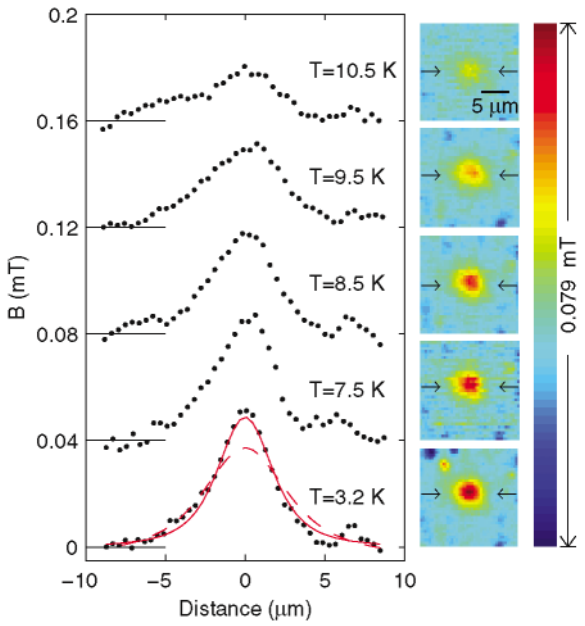

FIG. 4 (color). Hall probe images of a fluxoid in $YBa_2Cu_3O_{6.35}$ while cooling below $T_c = 12.7$ K. A linear fitted background has been subtracted. The bright and dark spots in the upper left of the 3.2 K image and elsewhere are understood as the Hall probe interacting with the electric field of charges on the sample surface. Cross sections, as indicated by the arrows, are shown offset by 0.04 mT for clarity. The FWHM decreases from 5.3 ± 0.3 μm at 10.5 K to 4.0 ± 0.3 μm at 3.2 K. The red lines are from 2D fits to the fluxoid with Φ set at $h/2e$ (solid line) and h/e (dashed line).

The $h/2e$ flux quantization was best established by the SQUID measurements, supplemented by the Hall probe to study temperature dependence. For consistency, we also used integration and fits to determine Φ of fluxoids in the Hall probe images. The integration had a large error associated with the fluxoid signal dropping into the noise quickly, potentially losing tenths of a flux quantum. Single fluxoid integration gave $\Phi = 0.7$ to 0.9 $h/2e$ in the near-optimally doped sample, where fluxoids are known to be $h/2e$, and $\Phi = 0.6$ to 0.8 $h/2e$ in the $x = 0.35$ sample for $T \lesssim 10$ K. In both cases, conservatively estimating the error in background determination to be its standard deviation gives an error $<0.6\ h/2e$ for Φ, and estimating a maximum error of 20% in the scanner area calibration gives an error 0.13 $h/2e$. Hall probe images of isolated fluxoids were also fit in two dimensions to Eq. (1) with free parameters $(z + \lambda_{ab})$, Φ, and a planar background. The best fits in the $x = 0.35$ sample gave total flux Φ primarily from 0.8 to 1.1 $h/2e$ for $T < 10$ K, and from 0.6 to 1.0 $h/2e$ for ~11 K. Systematic errors dominate, such as the high correlation between the parameters $(z + \lambda_{ab})$ and Φ, the planar background fit, and the validity of the model near T_c. An estimate of $\pm 0.2\ \mu$m for the error in $(z + \lambda_{ab})$ gives error bars $\leq 0.11\ h/2e$ for Φ, while the latter sources of error are more difficult to quantify. Fits with Φ fixed at $h/2e$ and at h/e clearly show $h/2e$ as the better fit (Fig. 4). In all, we observed 60 fluxoids with the Hall probe in the very underdoped YBCO.

The Hall probe images show apparent fluxoid spreading in $YBa_2Cu_3O_{6.35}$ [Fig. 3(b)] that may be due to a penetration depth that is not negligible compared to the 2 μm Hall probe. Alternative hypotheses include fluxoid bending, fast fluxoid motion confined to a micronscale region, or a non-superconducting layer on the crystal surface. The images in Fig. 4 show the temperature dependent fluxoid spreading in the very underdoped YBCO, consistent with a $\lambda_{ab}(T)$ that increases with temperature. The FWHM of a fluxoid image in the $x = 0.95$ sample is 3.0 ± 0.3 μm (resolution limited), while in the $x = 0.35$ sample it is 4.0 ± 0.3 μm at 3.2 K and 5.3 ± 0.3 μm at 10.5 K. From these numbers, and from the 2D fits with $(z + \lambda_{ab})$ as a free parameter, we interpret the major source of fluxoid spreading in the $x = 0.35$ YBCO as a penetration depth $\lambda_{ab} \gtrsim 1\ \mu$m which increases with temperature. This inferred λ_{ab} is somewhat larger than expected from higher-T_c extrapolations [21]. A more thorough and quantitative study of the penetration depth as a function of doping in underdoped cuprates would be possible with higher-resolution Hall probes.

Overall, we saw no h/e fluxoids in SQUID and Hall probe images of more than 170 fluxoids in $YBa_2Cu_3O_{6.35}$. This result sets limits on scenarios of spin-charge separation; in particular, we set an upper limit on the vison energy in the Senthil-Fisher formulation. They propose that $E_{\text{vison}} \approx k_B T^*$ (per layer) [8,22]. In the

usual Ginzburg-Landau theory, the energy per unit length of an $nh/2e$ fluxoid is given by $E^{nh/2e} = E_{\rm sf}^{nh/2e} + E_{\rm core}^{nh/2e}$, where

$$E_{\rm sf}^{nh/2e} = \frac{4\pi}{\mu_0}\left(\frac{nh/2e}{4\pi\lambda_{ab}}\right)^2 \ln(\lambda_{ab}/\xi) \qquad (2)$$

is the superfluid energy, n is an integer, ξ is the coherence length, and $E_{\rm core}$ is small compared to $E_{\rm sf}$ [23]. The vison can be cast as an excess core energy for an $h/2e$ fluxoid [8]. Thus we write $E^{h/2e} = E_{\rm sf}^{h/2e} + E_{\rm core} + E_{\rm vison}$, while $E^{h/e} = 4E_{\rm sf}^{h/2e} + E_{\rm core}$. The most natural interpretation of our observations of only $h/2e$ fluxoids is that $2E^{h/2e} < E^{h/e}$, and therefore $E_{\rm vison} < E_{\rm sf}^{h/2e}$ (neglecting pinning energy [24]). Conservatively using $\lambda_{ab} \approx 1\ \mu$m and taking $\ln(\lambda_{ab}/\xi) \approx 5$, we set an upper limit on the excess core energy associated with an $h/2e$ fluxoid: $E_{\rm vison}/k_B < 60$ K [25].

In the context of the Senthil-Fisher predictions, the significance of this upper limit depends on the exact value of T^*, which will be difficult to measure in these very underdoped samples because the dopant oxygens disorder above room temperature. Early NMR measurements indicate that T^* exceeds 300 K in $YBa_2Cu_3O_{6.48}$ [26]. A more recent interpretation of the T^* energy scale indicates values as high as 500–700 K in very underdoped samples [27]. Thus our upper bound on the vison energy is much below the predicted value. To reconcile this result with the predictions would require a superconducting transition which is strongly first order [5,8], or a theoretical model of fluxoid formation that does not permit h/e fluxoids even when they are energetically preferred [8]. We tested one such model by imaging fluxoids after cooling just below T_c. Senthil and Fisher also proposed an ingenious experiment to address the dynamics issue by trapping a vison in a hole in a cuprate cylinder [22]. These experiments are underway [28,29].

In the overall context of cuprate superconductivity, this work has extended experimental studies of single magnetic flux quanta into a new part of the phase diagram which was first theoretically explored a decade ago [5,6]. Further fluxoid imaging in these very underdoped samples will allow the determination of single fluxoid dynamics and energetics, as well as measurements of the absolute value of the magnetic penetration depth as a function of temperature and doping.

We thank Subir Sachdev, Matthew P. A. Fisher, and Senthil Todadri for inspirational discussions, and David Kisker at IBM for the GaAs/AlGaAs heterostructure used for the Hall probes. Work at Stanford was supported by the Sloan Foundation and by NSF Grant No. DMR-9875193. J. C. W. was supported by DoD, B. W. G. by NSERC, and work at UBC was supported by CIAR and NSERC of Canada.

*To whom correspondence should be addressed.
Email address: kmoler@stanford.edu

[1] B. S. Deaver, Jr., and W. M. Fairbank, Phys. Rev. Lett. **7**, 43 (1961).
[2] C. E. Gough *et al.,* Nature (London) **326**, 855 (1987).
[3] P. W. Anderson, Science **235**, 1196 (1987).
[4] S. A. Kivelson, D. S. Rokhsar, and J. P. Sethna, Europhys. Lett. **6**, 353 (1988).
[5] S. Sachdev, Phys. Rev. B **45**, 389 (1992).
[6] N. Nagaosa and P. A. Lee, Phys. Rev. B **45**, 966 (1992).
[7] N. Nagaosa, J. Phys. Soc. Jpn. **63**, 2835 (1994).
[8] T. Senthil and M. P. A. Fisher, cond-mat/0011345.
[9] T. Senthil and M. P. A. Fisher, Phys. Rev. B **62**, 7850 (2000).
[10] R. Moessner, S. L. Sondhi, and E. Fradkin, cond-mat/0103396.
[11] R. Liang, D. A. Bonn, and W. N. Hardy, Physica (Amsterdam) **304C**, 105 (1998).
[12] R. Liang, D. A. Bonn, and W. N. Hardy (unpublished).
[13] B. W. Veal *et al.,* Phys. Rev. B **42**, 4770 (1990).
[14] B. W. Gardner *et al.,* Rev. Sci. Instrum. **72**, 2361 (2001).
[15] J. Pearl, J. Appl. Phys. **37**, 4139 (1966).
[16] A. M. Chang *et al.,* Appl. Phys. Lett. **61**, 1974 (1992).
[17] V. G. Kogan, A. Yu. Simonov, and M. Ledvij, Phys. Rev. B **48**, 392 (1993).
[18] J. R. Kirtley, V. G. Kogan, J. R. Clem, and K. A. Moler, Phys. Rev. B **59**, 4343 (1999).
[19] The calculated field B_z for $r = 0$ and $z = \lambda_{ab}$ is only 16% greater for the monopole model compared to the full model. This error will be less for our SQUID images, since they are a convolution of the $8 \times 8\ \mu$m^2 pickup loop with the fluxoid field.
[20] D. N. Basov *et al.,* Phys. Rev. Lett. **74**, 598 (1995).
[21] Y. J. Uemura *et al.,* Phys. Rev. Lett. **62**, 2317 (1989).
[22] T. Senthil and M. P. A. Fisher, Phys. Rev. Lett. **86**, 292 (2001).
[23] M. Tinkham, *Introduction to Superconductivity* (McGraw-Hill, New York, 1996), 2nd ed., p. 153.
[24] With fluxoid pinning, $E^{nh/2e}$ has an additional term $-E_{\rm pin}^{nh/2e}$. Pinning potentials in high purity crystals may arise from small spatial variations in the doping. $E_{\rm pin}$ of a traditional fluxoid should be at most $\sim E_{\rm core}$, while here $E_{\rm pin}^{h/2e}$ could include a vison contribution $E_{\rm pin}^{\rm vison}$. Since in theory $E_{\rm vison} \approx k_B T^*, E_{\rm pin}^{\rm vison}$, due to doping variations, should be much smaller than $E_{\rm vison}$. Thus our energy balance expression becomes $E_{\rm vison} - E_{\rm pin}^{\rm vison} \approx E_{\rm vison} < E_{\rm sf}^{h/2e}$ as before.
[25] $E_{\rm vison}/k_B < 120$ K if there is one vison per unit cell instead of per copper-oxide plane.
[26] H. Alloul, T. Ohno, and P. Mendels, Phys. Rev. Lett. **63**, 1700 (1989).
[27] J. L. Tallon and J. W. Loram, Physica (Amsterdam) **349C**, 53 (2001).
[28] D. A. Bonn *et al.* Nature (London) (to be published).
[29] J. R. Kirtley *et al.* (unpublished).